Theor Chem Acc (2007) 118:357–362
DOI 10.1007/s00214-007-0268-8

REGULAR ARTICLE

DFT studies of the phosphinidene derivative HPNaF and its insertion reaction with R–H(R=F, OH, NH_2, CH_3)

**Xiaojun Tan · Weihua Wang · Ping Li ·
Xiuli Yang · Gengxiu Zheng · Yuxiang Ma ·
Zhuangdong Yuan**

Received: 12 December 2006 / Accepted: 30 January 2007 / Published online: 10 March 2007

Abstract The formations of the phosphinidene derivative HPNaF and its insertion reactions with R–H (R=F, OH, NH_2, CH_3) have been systematically investigated employing the density functional theory (DFT), such as the B3LYP and MPW1PW91 methods. A comparison with the results of MP2 calculations shows that MPW1PW91 underestimates the barrier heights for the four reactions considered. Similarly, the same is also true for the B3LYP method depending on the selected reactions, but by much less than MPW1PW91, where the barrier heights of the four reactions are 25.2, 85.7, 119.0, and 142.4 kJ/mol at the B3LYP/6-311+G* level of theory, respectively. All the mechanisms of the four reactions are identical to each other, i.e., an intermediate has been located during the insertion reaction. Then, the intermediate could dissociate to substituted phosphinidane(H_2RP) and NaF with a barrier corresponding to their respective dissociation energies. Correspondingly, the reaction energies for the four reactions are −92.2, −68.1, −57.2, and −44.3 kJ/mol at the B3LYP/6-311+G* level of theory, respectively, where both the B3LYP and MPW1PW91 methods underestimate the reaction energies compared with the MP2 results. The linear correlations between the calculated barrier heights and the reaction energies have also been observed. As a result, the relative reactivity among the four insertion reactions should be as follows: H–F > H–OH > H–NH_2 > H–CH_3.

Keywords Phosphinidene derivative (HPNaF) · Insertion reaction · Density functional theory (DFT)

1 Introduction

Reaction characters of monovalent hydrides HX(X=C, Si, B) with some small molecules attract much attentions because they play an important role in the chemical reactions involved in atmospheric chemistry, chemical catalysis, combustion, and quantum chemistry [1–4]. Recently, as one of the key intermediates in the hydrogenation of phosphorus to H_3P, the HP radical is being of interest both experimentally and theoretically in the field of interstellar chemistry, elemental chemistry, and organic metal chemistry [5,6]. The potential energy surfaces for the addition and insertion reactions of singlet phosphinidene with ethylene had been characterized by using ab initio molecular orbital theory including electron correlation [7]. The insertion reaction of phosphinidene ^{1}PH into H_2O, H_2S, HF, and HCl had also been studied by ab initio molecular orbital theory [8]. It has been shown previously that the ground state electronic configuration of compounds such as HP, FP or ClP consists mainly of a triplet phosphorus center interacting with the rest of the molecular [9–16]. Yin et al. [17] had studied the temperature influences on the insertion

X. Tan · X. Yang · G. Zheng · Y. Ma
College of Chemistry and Chemical Engineering,
University of Jinan, Jinan 250022, China

W. Wang · P. Li (✉)
Department of Chemistry, Qufu Normal University,
Qufu 273165, China
e-mail: lpsdu@sdu.edu.cn

P. Li
Institute of Theoretical Chemistry, Shandong University,
Jinan 250100, China

Z. Yuan
Department of Chemistry, Teacher's College of Jining,
Qufu 273155, China

reactions of singlet phosphinidenes XP(X=H, Li, F, Cl, OH, SH) with polar hydrogen chloride. Pierini et al. [18] reported the proton affinities of phosphinidene employing the AM1 and PM3 methods. Additionally, the molecular properties and the valence state energies of HP were calculated by Park using ab initio effective valence shell Hamiltonian methods [19].

As important reaction intermediates, the geometries and reaction activities of the alkali metal halides complexes of carbene, silylene, and nitrene, have been well characterized. Similarly, phosphinidenoid can be also formed between phosphinidene and alkali metal halides. For example, Lu et al. [20] had found that HPXF(X=Li, Na) is a superior electrophilic intermediate to free phosphinidene in selectivity and controlability. However, to our best knowledge, the reaction activities of HPNaF, such as its insertion reaction with other small molecules, have not been investigated systematically.

To better understand the nature of the insertion reaction between the phosphinidenoid and the asymmetrical bond, in the present study, the phosphinidene derivative HPNaF as well as its insertion reaction with R–H (R=F, OH, NH_2, CH_3) has been systematically investigated using the density functional theory as well as the MP2 method. Hopefully, the detailed mechanisms of the insertion reactions are expected to fill a void in the available data for the corresponding phosphinidenoid addition complexes and insertions into the R–H bond of solvent molecules.

2 Calculation method

All the initial geometries have been fully optimized using the B3LYP and MPW1PW91 density functional methods in conjunction with the 6-311+G* basis set followed by the frequency analyses to confirm the nature of the minima and transition states [21]. To investigate the efficiency of the both density functional methods in calculating the barrier heights, MP2/6-311+G* level of theory has also been performed to establish a benchmark for comparison. Furthermore, to explore the influences of the basis set on the relevant energy properties, a larger basis set Aug-cc-pVTZ including the diffuse and polarization functions has also been employed, where the corresponding MP2 calculations are too expensive to perform to our best computational ability. Additionally, intrinsic reaction coordinate (IRC) calculations have also been performed to further validate the calculated transition states connecting reactants and products. For the sake of simplicity, all the energy properties mentioned below, such as reaction energy and barrier height, have been corrected with zero-point vibrational energy (ZPVE) corrections if not noted otherwise.

All the calculations have been performed using Gaussian 98 programs [22].

3 Results and discussion

As mentioned above, full geometry optimizations suggest that the different levels of theory can give similar results in the structural characteristics for the considered species. On the other hand, the calculated energy properties are different more or less as mentioned below. Most importantly, the reactive activities among the four reactions considered are consistent with each other at all the levels of theory. Thus, for the sake of simplicity, the following discussions are based on the results of the B3LYP/6-311+G* level of theory if not noted otherwise.

3.1 The characteristics of HPNaF

As displayed in Fig. 1, two singlet states and one triplet state have been located on their corresponding poten-

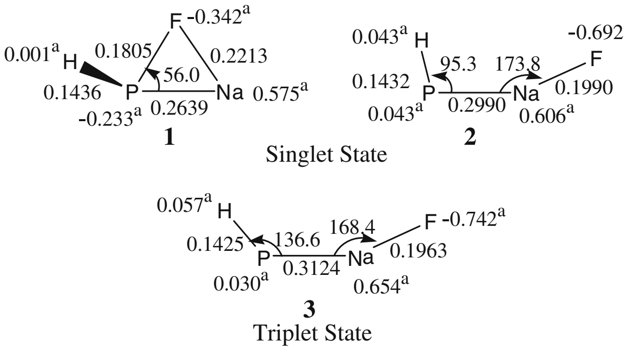

Fig. 1 The calculated geometries and Mulliken populations (denoted as [a]) of complex HPNaF, where the bond length and bond angle are in nm and degree, respectively

Table 1 The calculated relative energies (in kJ/mol) for the three complexes **HPNaF** at different levels of theory

HPNaF	Complex 1	Complex 2	Complex 3
MP2/6-311+G*[a]	0.0	201.6	62.9
B3LYP/6-311+G*	0.0	204.8	98.0
MPW1PW91/6-311+G*	0.0	225.1	95.9
B3LYP/Aug-cc-pVTZ	0.0	218.3	114.1
MPW1PW91/Aug-cc-pVTZ	0.0	240.1	114.3

All the results have been considered ZPVE corrections

[a] All the electrons have been included in the correlation calculation

tial energy surface, respectively. As shown in Table 1, all the levels of theory suggest that the complex **1** is the most stable one followed by the complexes **3** and **2**, where the relative energies for the latter two complexes are 98.0 and 204.8 kJ/mol relative to complex **1** at the B3LYP/6-311+G* level of theory, respectively. Here, compared with the results of MP2, both the B3LYP and MPW1PW91 methods overestimate the relative stability of complex **1** more or less. Similarly, the same is also true when the basis set is changed from 6-311+G* to Aug-cc-pVTZ for both density functional methods. Additionally, MPW1PW91 method underestimates the stability of complex **2** relative to that of B3LYP. On the other hand, both density functional methods give consistent results for the triplet complex **3** at the Aug-cc-pVTZ basis set.

For the most stable singlet and triplet HPNaF complexes, the corresponding formation processes can be described as follows. As shown in Fig. 2, in the singlet state, two pairs of electrons occupy both σ orbitals of HP and there is another empty *p* orbital left. Then, the Na and F atoms in NaF can interact with the σ and *p* orbitals of the HP, respectively, resulting in the formation of the three-membered ring structure. Here, there are charge transfers from the F atom to the *p* orbital of HP, leading to the reduction of the electron density of F atom. At the same time, the dative bond can be formed between the electropositive Na atom and the empty *p* orbital of HP. As a result, there should be a electronic circle of F → P → Na → F, resulting in the stabilization of the complex **1** relative to other complexes. Additionally, as can be seen from the calculated dihedral angle of 91.1°, complex **1** possesses a nonplanar structure.

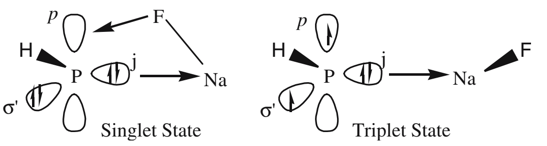

Fig. 2 The complexation processes between HP and NaF in the singlet and triplet states

As for the triplet HPNaF, two single electrons occupy the σ' and *p* orbitals besides a pair of electrons occupying the σ orbital of HP. Similar to that of the singlet case, a dative bond can also be formed between the electropositive Na atom and the empty *p* orbital of HP except that the charge transfer can not occur from F atom to the *p* orbital of HP, resulting in the larger electron density on F atom. At the same time, the angle of A(PNaF) is 168.4° rather than 180° due to the repulsion interaction of the electron in the σ' orbital, resulting in the formation of the coplanar and nonlinear geometry.

3.2 The structures and energies of the transition states in the insertion reactions

As mentioned above, the singlet HPNaF complex **1** is the most stable among the considered complexes. Thus, the representative complex **1** has been selected for further study of the insertion reactions between HPNaF and R–H (R=F, OH, NH_2, CH_3). Obviously, as displayed in Fig. 1, there is an exposed space that can be attacked by nucleophiles or electrophiles under the P atom. Thus, the insertion reaction between HPNaF and R–H should occur in this space.

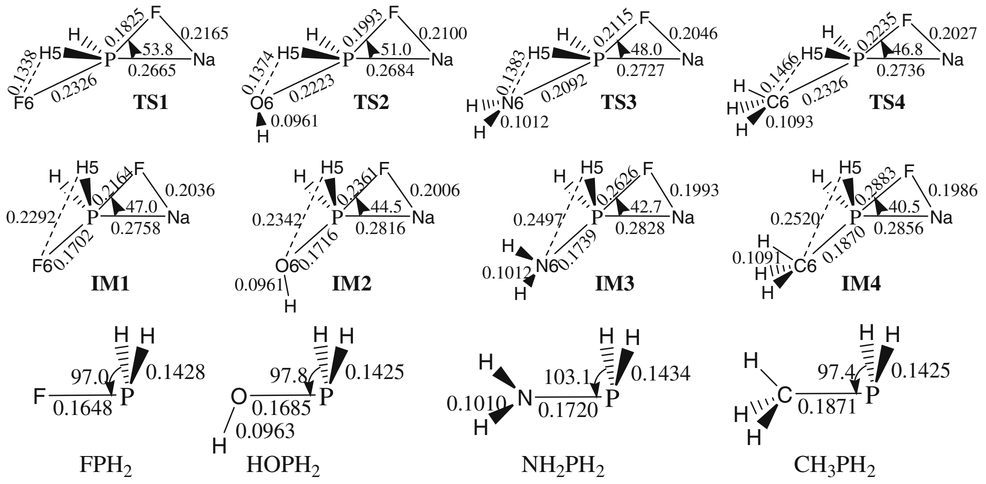

Fig. 3 Optimized structures of TSs, intermediates, and products, where the bond length and bond angle are in nm and degree, respectively

As displayed in Fig. 3, the calculated transition states in the insertion reactions have the similar structures. Here, the calculated unique imaginary frequencies are 1095.69i, 1409.45i, 1609.79i, and 1256.85i cm^{-1} for **TS1**, **TS2**, **TS3**, and **TS4** at the B3LYP/6-311+G* level of theory, respectively. Compared with the isolated HPNaF, the bond distances between P and F have been slightly elongated by about 0.0020, 0.0128, 0.0310, and 0.0430 nm when R is F, OH, NH_2, and CH_3, respectively. Obviously, the larger the electronegativity of R is, the less the change of the bond distances between P and F. On the other hand, the bond distance of R–H has been elongated significantly to 0.1338, 0.1374, 0.1383, and 0.1466 nm, respectively. Thus, in these transition states, the R–H bond is to be broken and a new P–H bond is to be formed simultaneously.

As displayed in Table 2, all the calculated barrier heights employing the B3LYP method are larger than those of the MPW1PW91 method. Moreover, all of them increase when the basis set changes from 6-311+G* to Aug-cc-pVTZ, depending on the selected reactions. For example, the barrier height increases by about 14.4–15.2 kJ/mol for R=F case with the increasing of the basis sets. However, the increment is only about 1.0–1.2 kJ/mol for the $R = CH_3$ reaction. On the other hand, compared with the MP2/6-311+G* level of theory, both the density functional methods underestimate the barrier heights except the selected reactions at the B3LYP/Aug-cc-pVTZ level of theory. Here, for the reactions of R=OH, NH_2, and CH_3, the barrier heights at the B3LYP/Aug-cc-pVTZ level of theory are larger about 0.2, 6.8, and 1.6 kJ/mol than those at the MP2/6-311+G*, respectively. Overall, the results of B3LYP method are much closer to those of the MP2 method than MPW1PW91 in the present study. Most importantly, the relative orders of the barrier heights are consistent with each other at all of the levels of theory employed here, that is, $R = F < R = OH < R = NH_2 < R = CH_3$.

3.3 The structures and energies of the intermediates and products in the insertion reactions

As displayed in Fig. 3, four intermediates have been located in the processes of the insertion reactions. Obviously, all of them have similar bipyramidal structures formed between the P atom and its adjacent atoms, where the heavy atoms in the R and F atoms are located at the two vertices of the bipyramid. Compared with the isolated R–H, the R–H bonds have been elongated significantly by about 0.1364, 0.1379, 0.1483, and 0.1429 nm, respectively, implying the broken of the R-H bond. At the same time, the distances between P and R atoms have been decreased significantly. For example, the corresponding bond lengths are 0.1702 ($R = F$), 0.1716 ($R = OH$), 0.1739 ($R = NH_2$), and 0.1870 nm ($R = CH_3$), respectively. Compared with the corresponding distances in the transition states, they have been shortened by 0.0674, 0.0507, 0.0353, and 0.0436 nm, respectively, suggesting the formations of the new P–R bonds.

The net charges on Na (F) are 0.709 (−0.583), 0.689 (−0.649), 0.684 (−0.696), and 0.637 (−0.711) when R=F, OH, NH_2, and CH_3, respectively. Thus, the intermediates should be a strong ionic complex, which can be

Table 2 Reactive energies of reactants, TSs, intermediates, and products (in kJ/mol) obtained at different levels of theory

Species	R=F	R=OH	$R = NH_2$	$R = CH_3$
HPNaF + RH	0.0	0.0	0.0	0.0
TS				
MP2/6-311+G*^{a}	43.2	95.0	120.3	141.8
B3LYP/6-311+G*	25.2	85.7	119.0	142.4
MPW1PW91/6-311+G*	23.3	79.7	108.4	130.9
B3LYP/Aug-cc-pVTZ	39.6	95.2	127.1	143.4
MPW1PW91/Aug-cc-pVTZ	38.5	90.1	117.3	132.1
IM				
MP2/6-311+G*^{a}	−168.0	−127.9	−116.5	−102.3
B3LYP/6-311+G*	−168.8	−118.8	−97.3	−78.6
MPW1PW91/6-311+G*	−174.1	−126.2	−106.9	−90.4
B3LYP/Aug-cc-pVTZ	−150.3	−103.3	−82.3	−66.1
MPW1PW91/Aug-cc-pVTZ	−152.6	−107.7	−88.9	−75.5
$RPH_2 + NaF$				
MP2/6-311+G*^{a}	−92.6	−76.9	−72.7	−62.3
B3LYP/6-311+G*	−92.2	−68.1	−57.2	−44.3
MPW1PW91/6-311+G*	−88.2	−69.3	−62.9	−53.5
B3LYP/Aug-cc-pVTZ	−77.3	−54.1	−43.3	−33.2
MPW1PW91/Aug-cc-pVTZ	−70.4	−52.5	−46.3	−40.4

All the results have been considered ZPVE corrections

[a] All the electrons have been included in the correlation calculation

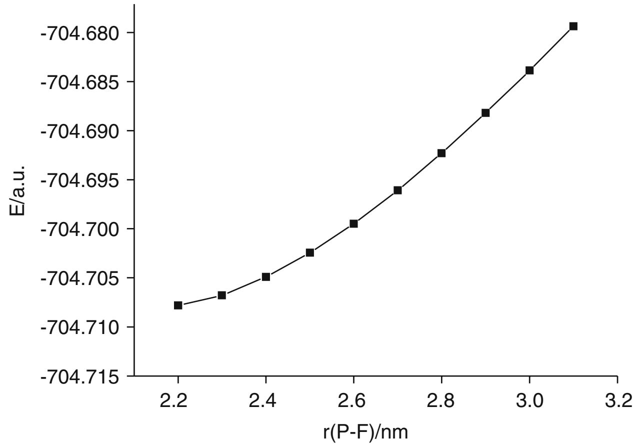

Fig. 4 Energy changes in the dissociation process of **IM1** for the HPNaF–HF system along with the distance of P–F

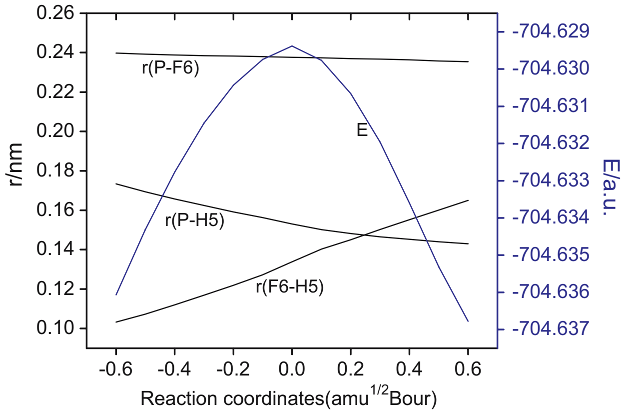

Fig. 5 The changes of energies and bond distances along the reaction coordinates

Table 3 Population analyses for the selected atoms in the HPNaF–HF system along the reaction coordinates at the B3LYP/6-311+G* level of theory

Reaction coordinates	P	F6	H5	F2	Na
−0.6	−0.382	−0.410	0.368	−0.294	0.659
−0.5	−0.360	−0.427	0.357	−0.294	0.663
−0.4	−0.333	−0.446	0.343	−0.295	0.667
−0.3	−0.303	−0.468	0.328	−0.296	0.671
−0.2	−0.274	−0.490	0.324	−0.297	0.675
−0.1	−0.242	−0.513	0.300	−0.298	0.679
0.0	−0.205	−0.541	0.284	−0.300	0.683
0.1	−0.170	−0.566	0.269	−0.302	0.687
0.2	−0.147	−0.583	0.259	−0.304	0.689
0.3	−0.125	−0.598	0.250	−0.306	0.690
0.4	−0.107	−0.609	0.242	−0.308	0.691
0.5	−0.091	−0.618	0.234	−0.310	0.692
0.6	−0.076	−0.625	0.227	−0.314	0.693

regarded as HPR, F^-, and Na^+ three fragments. With the increasing of the distance between P and F, the intermediates can be dissociated to H_2PR and NaF. To investigate this dissociation process, the potential energy curve for the **IM1** has been constructed along the distance between the P and F atoms. As displayed in Fig. 4, the energy of the system increases continuously with the increasing of the P-F distance qualitatively. Thus, the dissociation process should be a barrier process, where the corresponding barrier height is its dissociation energy.

Additionally, as shown in Table 2, compared with the reactants, the four intermediates have been stabilized by about 168.8 (R=F), 118.8 (R=OH), 97.3 ($R = NH_2$), and 78.6 kJ/mol ($R = CH_3$) at the B3LYP/6-311+G* level of theory, respectively. Obviously, all of the levels of theory give the consistent results. Correspondingly, the relative energies of the final products are −92.2, −68.1, −57.2, and −44.3 kJ/mol, suggesting that the whole reactions should be exothermic processes. Compared with the MP2 method, both the density functional methods underestimate the reaction energies. Moreover, all the reaction energies decrease when the basis set increases from 6-311+G* to Aug-cc-pVTZ. As a result, the relative orders in reaction energies are as follows: $R = F > R = OH > R = NH_2 > R = CH_3$.

3.4 The mechanism of insertion reaction

Taking the process of inserting H–F bond as an example, IRC calculations have been performed on the basis of the calculated **TS1** to investigate the interactions between two reactants in the insertion process (see Fig. 5). Correspondingly, the charge distributions for the selected atoms along the reaction coordinates have been presented in Table 3.

As shown in Table 3 and Fig. 5, the charges of the P and F6 atom decrease and increase gradually when the insertion reaction proceeds. At the same time, the distance between them decreases gradually, suggesting the formation of the P–F6 bond. On the other hand, as for the bond lengths of F6–H5 and P–H5, they increase and decrease with the proceeding of the reaction, implying the break of the former and the formation of the latter, respectively.

Furthermore, a plot of the barrier heights (ΔE^*) versus the reaction enthalpy (ΔH) shows that ΔE^* varies linearly with ΔH for all the processes considered. Namely, as shown in Fig. 6, a linear correlation exists between ΔE^* and ΔH, $\Delta H = 0.3984\Delta E^* - 102.52$, where the correlation coefficient is 0.9972. Accordingly, the present results are also consistent with the prediction

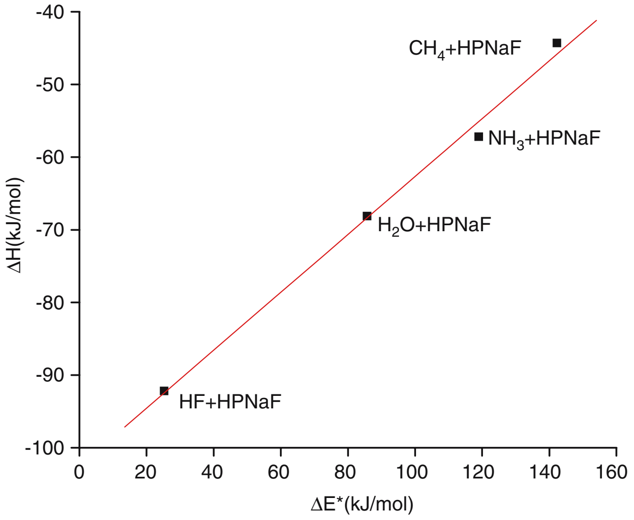

Fig. 6 The barrier height (ΔE*) versus the reaction enthalpy (ΔH) for the insertion of HPNaF with R–H (R=F, OH, NH$_2$, CH$_3$)

that the activation barrier should be correlated with the exothermicity of phosphinidene insertion [23].

3.5 The comparisons of the four insertion reactions

As shown in Table 2, at the B3LYP/6-311+G* level of theory, the calculated barrier heights are 25.2, 85.7, 119.0, and 142.4 kJ/mol for the four different inserting reactions of R=F, OH, NH$_2$, CH$_3$, respectively, exhibiting their different reactivities. Correspondingly, the calculated reaction energies are −92.2, −68.1, −57.2, and −44.3 kJ/mol, respectively. Thus, from the thermodynamic and kinetic viewpoints, the insertion reactions should occur easily in the order of H–F > H–OH > H–NH$_2$ > H–CH$_3$ under the same condition. This point is also consistent with the calculated charges on the H atoms of the nucleophiles, where the charges on the H atoms are 0.417, 0.369, 0.349, 0.233 in HF, H$_2$O, NH$_3$, and CH$_4$, respectively. Therefore, during the nucleophilic process, the relative reactivity among the four insertion reactions should be as follows: H–F > H–OH > H–NH$_2$ > H–CH$_3$.

4 Conclusions

In the present study, the formations of phosphinidene derivative HPNaF and its insertion reactions with R-H (R=F, OH, NH$_2$, CH$_3$) have been systematically investigated employing the B3LYP and MPW1PW91 density functional methods as well as the MP2 method. Generally, compared with the MP2 method, both the B3LYP and MPW1PW91 methods underestimate the barrier heights for the four reactions depending on the special systems, where the barrier heights of the four reactions are 25.2, 85.7, 119.0, and 142.4 kJ/mol at the B3LYP/6-311+G* level of theory, respectively. Similarly, the same is also true for the calculated reaction energies. All the mechanisms of the four reactions are identical to each other, i.e., an intermediate has been located during the insertion reaction. Then, the intermediate could dissociate to the substituted phosphinidane (H$_2$RP) and NaF with a barrier corresponding to the dissociation energies. Moreover, the calculated barrier heights are correlated linearly with the reaction enthalpies. As a result, the relative reactivity among the four insertion reactions should be as follows: H–F > H–OH > H–NH$_2$ > H–CH$_3$. Hopefully, the present results are expected to fill a void in the available data for the study of the interactions between the phosphinidene derivatives and the molecules possessing the R-H characteristics.

Acknowledgments We are highly grateful to the reviewer for his excellent suggestions to improve the presentation of the results.

References

1. Markus M, Roth P, Just T (1996) Int J Chem Kinet 28:171
2. Jasinski JM, Becerra R, Walsh R (1995) Chem Rev 95:1203
3. Bauer SH (1996) Chem Rev 96:1907
4. Schlegel HB, Baboul AG, Harris SJ (1996) J Phys Chem 100:9774
5. Partrick C, Amel G, Daniel M (1996) J Mol Struct(THEOCHEM) 369:85
6. Yin P, Wang ZL, Bai ZP (2001) Chem Phys 264:1
7. Gonbeau D, Pfister G (1987) Inorg Chem 26:1799
8. Sudhakar PV, Lammertsma K (1991) J Org Chem 56:6067
9. Marinetti A, Mathey F, Fischer J (1982) J Am Chem Soc 104:4484
10. Mercier F, Deschamps B, Mathey F (1989) J Am Chem Soc 111:9098
11. Lammertsma K, Chand P, Yang AW (1988) Organometallics 7:1875
12. Barclay VJ, Wright JS (1988) Chem Phys 121:381
13. Ahlrichs R, Schunk S (1988) Angew Chem 100:418
14. Curtiss LA, Ragahavachari K, Trucks GW (1991) J Chem Phys 94:7221
15. Peterson KA, Woods RC (1990) J Chem Phys 93:1876
16. Frison G, Mathey F, Sevin A (1998) J Organomet Chem 570:225
17. Yin P, Zheng H, Yin G (2005) J Mol Struct(THEOCHEM) 755:203
18. Pierini AB, Duca JS (1993) Int Quantum Chem 48:343
19. Park JK, Sun H (1992) Chem Phys Lett 195:469
20. Lu XH, Wang YX, Deng CH (1998) Chem J Chin Univ 4:617
21. Adamo C, Barone V (1998) J Chem Phys 108:664
22. Frisch MJ et al. (1998) Gaussian 98, Gaussian Inc., Pittsburgh, PA,
23. Pross A (1995) Theoretical and physical principles of organic reactivity. Wiley, Inc., USA